Accepted Manuscript

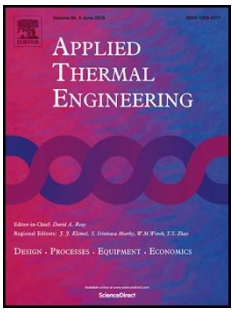

Title: A heat transfer correlation for transient vapor uptake of powdered adsorbent embedded onto the fins of heat exchangers

Author: Ang Li, Kyaw Thu, Azhar Bin Ismail, Kim Choon Ng

PII: S1359-4311(15)00977-1
DOI: http://dx.doi.org/doi: 10.1016/j.applthermaleng.2015.09.057
Reference: ATE 7049

To appear in: *Applied Thermal Engineering*

Received date: 20-6-2015
Accepted date: 20-9-2015

Please cite this article as: Ang Li, Kyaw Thu, Azhar Bin Ismail, Kim Choon Ng, A heat transfer correlation for transient vapor uptake of powdered adsorbent embedded onto the fins of heat exchangers, *Applied Thermal Engineering* (2015), http://dx.doi.org/doi: 10.1016/j.applthermaleng.2015.09.057.

A HEAT TRANSFER CORRELATION FOR TRANSIENT VAPOR UPTAKE OF POWDERED ADSORBENT EMBEDDED ONTO THE FINS OF HEAT EXCHANGERS

Ang Li, Kyaw Thu, Azhar Bin Ismail, Kim Choon Ng*

Highlights

- Detailed study on transient heat transfer of an adsorbent coated heat exchanger.
- Adsorbent-adsorbate interaction contributes 75% of the total thermal resistance.
- Transient local heat transfer deviates from the overall value due to thermal mass.
- A correlation for the transient local adsorption heat transfer coefficient.

ABSTRACT

We present a detailed study on the transient heat transfer phenomena of powdered-adsorbent mixed with an organic binder for adherence to the fins of a heat exchangers. The transient performance of such an adsorbent-heat exchanger configuration has significant application potential in the adsorption desalination plants and chillers but seldom addressed in the literature. An experiment is designed to measure the heat transfer for several adsorption temperatures under a single vapor component environment. Analysis on the experimental data indicates that the adsorbent-adsorbate interactions contribute about 75% of the total thermal resistances throughout the uptake processes. It is found that the initial local adsorption heat transfer coefficients are significantly higher than the average values due primarily to the thermal mass effect of the adsorbent–adsorbate interaction layers. From these experiments, a correlation for the transient local adsorption heat transfer coefficients is presented at the sub-atmospheric pressures and assorted application temperatures.

KEYWORDS

*Correspoinding author, E-mail : mpengkc@nus.edu.sg; and Kim.NG@kaust.edu.sa

Adsorption, thermal resistance, transient heat transfer correlation, silica gel

*Correspoinding author, E-mail : mpengkc@nus.edu.sg; and Kim.NG@kaust.edu.sa

NOMENCLATURE

Symbols

A	Area, [m^2]
Ad	Adsorption number, [-]
Bi	Biot number, [-]
C	Regression constant for adsorption isotherm model, [-];
Cp	Specific heat capacity, [kJ/kg.K]
d	Diameter, [m]
D_{so}	Pre-exponential factor for surface diffusion, [m^2/s]
E_a	Activation energy, [kJ/kmol]
E_c	Characteristic energy, [kJ/kg]
f	Friction factor, [-]
Fo	Fourier number, [-]
h_t	Local heat transfer coefficient, [W/m^2.K]
K	Pre-exponential constant of adsorption, [kPa^{-1}]
k	Thermal conductivity, [W/m.K]
M	Mass, [kg]
$\dot{m}$	Mass flow-rate, [kg/s]
Nu	Nusselt number, [-]
$NRMSE$	Normalized root mean square error to the mean experimental data
P	Pressure, [kPa]
P_s	Saturation Pressure, [kPa]
P_l	Longitudinal tube pitch, [m]
Pr	Prandtl number, [-]
P_t	Transverse tube pitch, [m]
$Q_{st,ads}$	Isosteric heat of adsorption, [kJ/kg]
q^*	Equilibrium adsorbate uptake, [kg/kg of adsorbent]
R	Universal gas constant, [kJ/kmol.K] ; thermal resistance, [K/W]
R^2	Coefficient of determination
Re	Reynolds number, [-]
R_{eq}	Equivalent radius to circular fins, [m]
R_p	Average radius of adsorbant particles, [m]
r	Radius, [m]
T	Temperature, [K]
t	Time, [s]; surface heterogeneity, [-]
U	Overall heat transfer coefficient, [kW/m^2.K]
v	Specific volume, [m^3/kg]

Greek Symbols

δ	Thickness, [m]
η	Surface efficiency of heat exchanger, [-]

κ	Diffusion constant in LDF model, [-]
ρ	Density, [kg/m^3]
ϕ	Pre-exponent constant in adsorption isotherm model, [-]
ψ	Temperature dimensionless number, [-]

Subscripts

ads	Adsorbent-adsorbate interaction layer
b	Binder or additive
cw	Cooling water
e	Evaporator
eff	Net effect
f	Liquid phase
fin	Heat exchanger fins
g	Gaseous phase
i	Inlet; inner
ini	Initial state
o	Outlet; outside
sg	Silica gel
tw	Tube wall
α	Adsorbate in adsorbed phase

1. INTRODUCTION

Adsorption/desorption cycle is widely used as a thermal vapor compressor in chiller [1, 2], desalination [3, 4], and gas storage applications [5, 6], owning to its green nature of being waste heat driven, environmental benign and elimination of major moving parts. The cycle is achieved by periodically cooling and heating solid adsorbents in a gas (known as adsorbate) surrounded environment, through fin-tube heat exchangers where the adsorbents are embedded between fins.

To date, however, the design of adsorbent embedded heat exchangers relies on designers' skilled art. Understanding and development of the adsorption heat transfer are rarely found in the literature. Many researchers simulate highly transient performance of adsorption /desorption beds by using a constant heat transfer coefficients [7-11]. Mayer *et al.* [12], Bjurström *et al.* [13], Tsotsas and Martin [14], Murashov and White [15], and recently Yan *et al*. [16] characterize the adsorption heat transfer by focusing on the thermal conductivity of the adsorbents. However, Freni *et al.* [17] pointed out that the thermal conductivities of the $CaCl_2/SiO_2$ and $LiBr/SiO_2$ composite sorbents was considerably affected by the amount water adsorbed. A constant conductivity value could yield error as big as 30% in the cooling power calculation of the adsorption chillers.

This encourages the authors of the present work to study in detail the transient adsorption heat transfer behaviors instead of the thermal conductivity of adsorbent [18-21] with motivations as follows. Firstly, the adsorption heat transfer processes are highly dynamic, accompanying with temporal variations of adsorbate uptake, heat flux and system temperature, etc., whereas the thermal conductivity measurement is normally conducted in steady state conditions. It is insufficient to quantify a transient process with steady state

values. Secondly, the adsorption processes involve several parallel phenomena, including heat generation from the phase change of the adsorbate, conduction through the adsorbent material, and convective interaction with the surrounding gases. The thermal conductivity only plays part of role in the overall processes. Last but not least, the measurement of the thermal conductivity cannot reveal the effect of the adsorbate mass transport, like uptake kinetics and diffusivity in the adsorbent, which are rather influential to the heat transfer processes. The transient heat transfer coefficient, in contrast, is measured in the conditions of industrial applications and able to accurately quantify the overall adsorption heat transfer processes.

2. EXPERIMENTAL SETUP AND PROCEDURES

An experimental apparatus was designed to study the transient adsorption heat transfer behaviour of silica gel in a single component environment, as schematically illustrated in Figure 1. A two-pass copper fin-tube heat exchanger is located in the adsorption chamber. Its total surface area is 0.066 m^2. The fins are coated by 37.4 g silica gel type RD powder using 3.3 adsorbent weight percent of hydroxyethyl cellulose (HEC) binder with an average coating thickness of 0.7 mm. The detailed dimensions and a pictorial view of the heat exchanger are shown in Figure 2. The temperature of the heat exchanger systems are measured by twelve element type thermistors (Omega™ 44031), out of which five thermistors record the silica gel layer temperatures in different locations. An illustration on how the beads of the thermistors are embedded into the silica gel layers is given in Figure 2(b). The beads have diameter of 2 mm. They are sandwiched by the adsorbent layers to ensure no contact with vapour flow and fin surface. This configuration eliminates the influence of surrounding structure to the measurement of the adsorbent-adsorbate interaction layer. Probe type

thermistors (Omega™ TH-10-44006-1/8-100-1) are used to measure the cooling water and evaporator temperatures. Both types of thermistors have accuracy of ± 0.1 ^{o}C and calibrated using a master thermometer with accuracy ± 0.025 ^{o}C. The evaporator and heat exchanger cooling water temperatures are maintained by water circulators. The pressure of the vessels are gauged by GEMS™ pressure transducer within ± 0.25 kPa precision to indicate the vacuum of the chambers. The vapour spaces are wrapped by heat tapes to prevent vapour condensation. Heat leak is minimized by applying insulation around the exposed tubing.

The water adsorption heat transfer measurement of the silica gel was conducted at several cooling water temperatures. Prior to each test, the silica gel was regenerated by circulating 90 ^{o}C hot water into the heat exchanger tubes, and operating the vacuum pump to extracts moisture desorbed from the adsorbent. After the silica gel is sufficiently dry and vacuum is established in the adsorption chamber, the cooling water is supplied to the heat exchanger. The adsorption processes were started when the system reaches steady state. The testing conditions of the experiment is summarized in Table 1. Heat leak of the adsorption chamber was quantified in the experimental conditions. It was tested by naturally cooling down the system from full regeneration conditions at 90 ^{o}C and vacuum. No adsorption / desorption is involved in the cooling process. Temperatures of the heat exchanger materials (tube, fins and silica gel layers), and the experiment room were recorded. The heat loss for a particular temperature difference between the heat exchanger and the room equals to the temporal temperature gradient of the heat exchanger thermal mass.

3. GOVERNING THEORIES

3.1.The Heat Transfer System

An adsorbent embedded heat exchanger consists of four thermal layers, i.e. adsorbent-adsorbate interaction, conduction through the fin, the tube wall, and convection between the inner tube wall and cooling water bulk flow. Each layer possesses not only thermal resistance, the thermal mass can neither be ignored in conjunction with the dynamic heat and mass transfer nature of an adsorption process. In particular, the adsorbent-adsorbate interaction layer involves several parallel events, including the phase change of the adsorbate that results in heat generation, the conduction through the adsorbent solids and vapor that fills up the void space, as well as the contact resistance in between the substances and metal fins. A separate analysis of each parallel phenomenon is rather complicated due to the interlacement among the phenomena and inhomogeneity at different locations. Hence, we propose a single term to study the net influence of all the parallel phenomena, named as local adsorption heat transfer coefficient, and defined as the amount of heat flux across the temperature difference between the fin surface and the average of the adsorbent-adsorbate interaction layer.

3.2.Overall Heat Transfer Coefficient

Due to the transient nature of the adsorption processes, the overall heat transfer coefficient (U) of the adsorbent embedded heat exchanger is calculated as below,

$$U\ (t) = \frac{\left[\dot{m} Cp\,(T_o - T_i)\right]_{cw}}{A\left(T_{ads} - T_{i,cw}\right)} \tag{1}$$

where T_{ads} denotes an average instantaneous temperature of the adsorbent-adsorbate layer. It is noted that in the right hand side of the equation, the value of T_{ads} and $T_{o,cw}$ are changing with respect to time.

3.3.Resistances of the Thermal Layers

3.3.1. Overall heat transfer resistance

Concerning transient heat transfer in each thermal layer, the net amount of heat passes through the layer is equal to the total entering heat minus the heat reserved in the layer's thermal mass. The temperature difference between boundaries of the layer in the heat transfer direction is created as the net heat flow is resisted by the thermal resistance. Particularly to the adsorbent-adsorbate interaction layer, the temperature difference is calculated from the following equation:

$$T_{ads} - T_{fin} = R_{ads} \cdot \left(Q_{eff} - M_{sg} Cp_{ads} \frac{dT_{ads}}{dt} \right) \tag{2}$$

where, the effective specific heat capacity of the adsorption system, Cp_{ads}, is,

$$Cp_{ads} = Cp_{sg} + qCp_{\alpha} + \frac{M_b}{M_{sg}} Cp_b \tag{3}$$

and, the amount of net heat entering the adsorbent-adsorbate system, Q_{eff}, is the total effect of heat of adsorption, vapor superheating and heat loss to the surrounding, and expressed as,

$$Q_{eff} = Q_{adsorption} + Q_{superheating} - Q_{loss}$$
$$= M_{sg}\frac{dq}{dt}Q_{st,ads} + M_{sg}\frac{dq}{dt}\left[h_g\left(T_e\right) - h_g\left(T_{ads}, P_e\right)\right] - M_{sg}\frac{dq}{dt}\tilde{Q}_{loss} \quad (4)$$

In the two equations above, the instantaneous uptake of the adsorbate q, the rate of uptake $\frac{dq}{dt}$, the heat of adsorption $Q_{st,ads,}$ and the adsorbed phase specific heat capacity of the adsorbate Cp_α are related to the characteristics of the adsorbent-adsorbate pair, and calculated using theories listed in Table 2. The superheating term, $Q_{superheating,}$ concerns the temperature raise of the vapor from the evaporator to the adsorption chamber. $\tilde{Q}_{loss}$ is normalized heat loss per unit mass of phase changing adsorbate from the total heat loss Q_{loss}.

Similar techniques are applied to the conduction layers in the fin and tube wall, as well as the convection layer in the cooling water. Incorporate with energy balance of the adsorption heat transfer process as written below,

$$Q_{cw} = Q_{eff} - M_{sg}Cp_{ads}\frac{dT_{ads}}{dt} - M_{fin}Cp_{fin}\frac{dT_{fin}}{dt} - M_{tw}Cp_{tw}\frac{dT_{tw}}{dt} \quad (5)$$

The overall transient thermal resistance can be obtained as below,

$$\frac{1}{U\left(t\right)A} = \frac{T_{ads} - T_{i,cw}}{Q_{cw}} = R_i + R_{tw}$$
$$+ R_{fin}\cdot\frac{Q_{eff} - M_{sg}Cp_{ads}\frac{dT_{ads}}{dt} - M_{fin}Cp_{fin}\frac{dT_{fin}}{dt}}{Q_{cw}} \quad (6)$$
$$+ R_{ads}\cdot\frac{Q_{eff} - M_{sg}Cp_{ads}\frac{dT_{ads}}{dt}}{Q_{cw}}$$

3.3.2. Convection near the Tube Inner Wall

The convection thermal resistance between the cooling water bulk flow and the circular tube inner wall is given by,

$$R_i = \frac{1}{h_{t,i} A_i} \tag{7}$$

For turbulent boundary layer formed near the tube inner wall at Reynolds number between 3000 and 10^6, Gnielinski's correlation can be applied to predict the value of $h_{t,i}$ [24, 25].

$$h_{t,i} = \frac{Nuk_{cw}}{d_i} \tag{8}$$

The Nusselt number *Nu* is calculated from an empirical relation,

$$Nu = \frac{(f/8)(Re-1000)}{1+12.7(f/8)^{1/2}\left(Pr^{2/3}-1\right)} \tag{9}$$

where, *f* is friction factor for a smooth wall given by Petukhov's formula

$$f = \left(0.79\ln(Re)-1.64\right)^{-2} \tag{10}$$

3.3.3. Conduction through the Tube Wall

The conduction thermal resistance through the tube wall is given by,

$$R_{tw} = \frac{r_o \ln\left(r_o/r_i\right)}{k_{tw} A_o} \tag{11}$$

3.3.4. Conduction through the Fins

The thermal resistance of the heat transfer in the fins is computed from the heat exchanger surface efficiency η by the following equation,

$$R_{fin} = \left(\frac{1}{\eta} - 1 \right) \cdot \frac{1}{h_{t,ads} A} \tag{12}$$

where, $h_{t,ads}$ represents the local adsorption heat transfer coefficient from the fin surface to the average of the adsorbent-adsorbate layer. For the plain fin-tube type heat exchanger, its heat transfer surface efficiency can be determined from Schmidt equations listed in Table 3 [26-28]. Hong and Webb [29] suggested that the Schmidt equation will give more than 5% error if $R_{eq}/r_o > 3$ and $\xi \left(R_{eq} - r_o \right) > 2$. Most of the practical applications, however, are well within the limits.

3.3.5. Adsorbent-Adsorbate Interaction Thermal Layer

Substituting the aforementioned thermal resistances into Equation 6 and invoking the energy balance in Equation 5, the effective thermal resistance of the adsorbent-adsorbate interaction layer can be obtained as,

$$R_{ads} = \frac{1}{h_{t,ads} A} = \frac{\left(\frac{1}{UA} - \frac{1}{h_{t,i} A_i} - \frac{r_o \ln \left(r_o / r_i \right)}{k_{tw} A_o} \right) Q_{cw}}{M_{fin} Cp_{fin} \frac{dT_{fin}}{dt} + \frac{1}{\eta} \left(Q_{cw} + M_{tw} Cp_{tw} \frac{dT_{tw}}{dt} \right)} \tag{13}$$

Rearranging Equation 12, $h_{t,ads}$ can be computed from the overall heat transfer coefficient, thermal masses and resistances of other thermal layers with established theories. Figure 3 summarizes the thermal resistances of the adsorbent embedded heat exchanger in a typical adsorption heat transfer process.

$$h_{t,ads} = \frac{M_{fin} Cp_{fin} \frac{dT_{fin}}{dt} + \frac{1}{\eta}\left(Q_{cw} + M_{tw} Cp_{tw} \frac{dT_{tw}}{dt} \right)}{\left(\frac{1}{U} - \frac{A}{h_{t,i} A_i} - \frac{A r_o \ln\left(r_o / r_i\right)}{k_{tw} A_o} \right) Q_{cw}} \quad (14)$$

4. RESULTS AND ANALYSIS

4.1.Overall Performance of the Heat Exchanger

The transient nature of adsorption heat transfer process comes from a decaying rate of mass transport as the adsorbate uptake approaches saturation. Due to the affinity of the silica gel to the water vapour, a strong driving force is created to migrate the vapour from evaporator to the solid surface, and release the heat of adsorption which is usually bigger than the latent heat of the adsorbate [23]. The heat is rejected to the cooling water circulating through the heat exchanger tubes. Figure 4 illustrates the temporal temperature difference between the adsorbent – adsorbate layer average and cooling water inlet at various cooling water temperatures. The values of the instantaneous overall heat transfer coefficient of the heat exchanger are computed and shown in Figure 5.

4.2.Resistances of Thermal Layers

Reynolds number in the experimental conditions is 3110 to 4200. The local adsorption heat transfer coefficient $h_{t,ads}$, is calculated by solving Equation 14 and the surface efficiency of

the heat exchanger η (shown in Table 3) simultaneously. Table 4 listed the specification of the heat exchanger.

The results of temporal surface efficiency of the heat exchanger during adsorption processes are shown in Figure 6. The efficiency increases with time and stabilizes at 95% after 150 s for all the cases. The deviation takes place in the early period of the processes in which a lower temperature delivers comparatively higher efficiency. Figure 7 shows the local adsorption heat transfer coefficient in the same conditions. However, an opposite trend with respect to temporal changes is evident between the local and overall values, and emphasized in Figure 8 using a typical cooling water inlet temperature of 30^{o}C. The local heat transfer rate is highest at the beginning of the process, whereas overall transfer rate is suppressed. This deviation implies that thermal inertia is encountered along the heat transfer path. To further investigate the deviation, it is necessary to understand the temporal thermal resistance of each layer.

Figure 9 illustrates the thermal resistance of each layer along the adsorption heat transfer path. The values for the fin and adsorbent-adsorbate layer include the thermal mass factor formulated in Equation 6. The cumulative value is the overall thermal resistance. As it is shown, the overall thermal resistance is as high as 0.81 K/W at the beginning of the adsorption process and gradually stabilizes to an average of 0.29 K/W after 150 s. Among the resistance of sublayers, the adsorbent-adsorbate interaction is dominant, followed by the convection in the cooling water, the conduction in the fin, and lastly tube wall. The adsorbent-adsorbate interaction and conduction in the fin contribute in average 0.255 K/W

and 0.0125 K/W in the steady-stage range. The cooling water convection and conduction in the tube wall keep relatively constant values with 0.056 K/W and 0.0002 K/W correspondingly throughout the process. The percentage contribution of each layer to the overall thermal resistance is plotted in Figure 10. It is noted that the fin counts three times higher of the contribution than the cooling water convection layer in the initial adsorption process. The proportion is, however, reversed after 150 s as the fin declines to 4.2%, and the latter rises to an average of 19.1%. A major contribution of 76.5% at the steady cooling processes is from the adsorbent – adsorbate interaction layer.

Despite the percentage contribution, the big variation on the thermal resistance of the adsorbent-adsorbate interaction and the fin layers also draws attention. This entails thermal inertia faced by both layers in the initial adsorption processes, and it is attributable to the thermal mass, as shown in Figures 11 and 12. The results indicate that most of the heat released in this period is stored in the thermal mass instead of transferring to the cooling water. This well explains the initial large deviation on heat transfer coefficient between the local adsorbant-adsorbate layer and the overall value, as well as the sharp increase of the adsorbent temperature in the same period. In addition, the effect of the thermal mass turns negative at the processes after 60 s when the adsorbent temperature reaches maximum. It compensates the heat transfer by reducing the net resistance of the adsorption layer, since the adsorbent cools down afterwards.

An uncertainty analysis is conducted to determine the accuracy of the measurements. The uncertainties of the sensors, data logging frequency, thermal mass effect of the thermistors and other bias errors are considered in the analysis. The results show that the measurement yields uncertainty 9.48%. It is noted that the delay caused by the thermistors' thermal mass is estimated from the time constant provided by the manufacturer. Its uncertainty is taken as five times of the time constant which produces the measured value well within the thermistor

tolerance. Adding the uncertainty of the data logging sampling frequency, the total time-related uncertainty is 0.045 s, which incurs 0.48% error to the heat transfer coefficient.

5. PREDICTION OF LOCAL ADSORPTION HEAT TRANSFER COEFFICIENT

5.1.Derivation of correlation

In the content below, effort is made to derive a transient correlation to predict the local adsorption heat transfer coefficient from heat exchanger geometries and adsorbent-adsorbate pair properties.

Figure 13 illustrates the heat flow direction on the heat exchanger during adsorption processes. The control volume is defined as the enclosed space occupied by the adsorbent material and adsorbed phase of the adsorbate. The local adsorption heat transfer coefficient is concerning the rate of heat flux across the temperature difference between the control volume and the fin surface, and based on the assumptions: 1) Adsorbent material is located evenly on the fins of the heat exchanger. 2) Adsorption takes place uniformly in the control volume. 3) Temperature variation in the control volume is negligible. 4) Heat transferred due to the direct contact of the adsorbent and the tube wall is omitted. Fin is the sole heat transfer path.

5) Heat loss to the surrounding is neglected. Concerning the energy balance on the control volume, the equation is,

$$\rho_{sg} A\delta_{sg} Cp_{ads} \frac{dT_{ads}}{dt} = \rho_{sg} A\delta_{sg} \frac{dq}{dt} Q_{st,ads} + h_{t,ads} A\left(T_{fin} - T_{ads}(t)\right) \tag{15}$$

Substitute the rate of uptake $\frac{dq}{dt}$ given in Table 1 into Equation 15,

$$\begin{aligned}\rho_{sg} A\delta_{sg} Cp_{ads} \frac{dT_{ads}(t)}{dt} = {} & \rho_{sg} A\delta_{sg} \kappa \left[q^* - q_{ini}\right] e^{-\kappa t} Q_{st,ads} \\ & + h_{t,ads} A\left(T_{fin} - T_{ads}(t)\right)\end{aligned} \tag{16}$$

Solve the adsorbent temperature T_{ads} with respect to time t with initial condition:

At $t = 0$, $T_{ads}(0) - T_{fin} = T_{ini} - T_{fin,ini}$,

where T_{ini} and $T_{fin,ini}$ are the initial temperature of the adsorbent and fins respectively upon the adsorption starts. Rearrange,

$$\begin{aligned}\frac{T_{ads}(t) - T_{fin}}{T_{ini} - T_{fin,ini}} = {} & \exp\left(\frac{-h_{t,ads}}{\rho_{sg}\delta_{sg} Cp_{ads}} t\right) \\ & + \frac{\rho_{sg}\delta_{sg}\kappa\left(q^* - q_{ini}\right) Q_{st,ads}}{\left(h_{t,ads} - \rho_{sg}\delta_{sg} Cp_{ads}\kappa\right)\left(T_{ini} - T_{fin,ini}\right)} \\ & \cdot\left[\exp(-\kappa t) - \exp\left(\frac{-h_{t,ads}}{\rho_{sg}\delta_{sg} Cp_{ads}} t\right)\right]\end{aligned} \tag{17}$$

Regroup the parameters by introducing dimensionless groups. Define Biot number:

$$Bi = \frac{h_{t,ads}\delta_{sg}}{k_{sg}} \tag{18}$$

Fourier number:

$$Fo = \frac{k_{sg}}{\rho_{sg}\delta_{sg}^{2} Cp_{ads}} t \tag{19}$$

And, the temperature dimensionless group:

$$\psi = \frac{T_{ads}(t) - T_{fin}}{T_{ini} - T_{fin,ini}} \tag{20}$$

Equation 17 can be simplified as:

$$\psi = \exp(-Bi \cdot Fo) + \frac{\frac{(q^{*} - q_{ini}) Q_{st,ads}}{Cp_{ads}(T_{ini} - T_{fin,ini})}}{\left(\frac{Bi \cdot Fo}{\kappa t} - 1\right)} \left[\exp(-\kappa t) - \exp(-Bi \cdot Fo)\right] \tag{21}$$

To further simply the equation, a new dimensionless group is introduced in the present work, namely adsorption number. It is defined as,

$$Ad = \frac{(q^{*} - q_{ini}) Q_{st,ads}}{Cp_{ads}(T_{ini} - T_{fin,ini})} \tag{22}$$

The numerator in this expression calculates the total heat of adsorption released from initiation of the adsorption till saturation. The denominator describes the amount of heat reserved in the adsorbent-adsorbate system from initiation to reach fin surface temperature. The ratio of the two quantities reflects the magnitude of the heat of adsorption being accumulated inside the adsorbent-adsorbate interaction layer during adsorption processes. Large adsorption number implies fast heat transfer out of the system.

Hence, the equation to predict the transient local adsorption heat transfer coefficient is,

$$\psi = \exp\left(-Bi \cdot Fo\right) + \frac{Ad}{\left(\frac{Bi \cdot Fo}{\kappa t} - 1\right)}\left[\exp\left(-\kappa t\right) - \exp\left(-Bi \cdot Fo\right)\right] \tag{23}$$

where, the transient local adsorption heat transfer coefficient $h_{t,ads}$ can be computed by solve the Biot number iteratively from the equation with the specification of the adsorbent coating and properties of the adsorbent-adsorbate pair. The first term on the right hand side of the equation describes the rate of natural convection out of the control volume. The difference between this phenomenon and the heat generation rate inside the control volume is indicated in the other term. The heat generation is due to the mass transport in which the adsorbate experiences phase change from gaseous to the adsorbed phase. Clearly, the temperature of the adsorbent-adsorbate system is determined by the competition of mass transport and the convective heat transfer out of the system. In addition, Equation 23 is qualified by the nature of the adsorption heat transfer process in which,

at $t = 0$, $\lim_{t \to 0}(\psi) = 1$, or $T_{ads} = T_{ini}$, and,

at $t = \infty$, $\lim_{t \to \infty}(\psi) = 0$, or $T_{ads} = T_{fin}$

5.2.Results

Equation 23 is implemented to predict the local adsorption heat transfer coefficient of the silica gel coated heat exchanger during adsorption at 25 - 40 ^{o}C cooling water. The results are validated with the experimental data stated in Section 4. The adsorption characteristic parameters of the silica gel-water pairs are summarized in Table 2. The parameters substituted in the calculation are summarized in Table 5 [30].

The results of the prediction from Equation 23 are illustrated in Figure 14. The predicted local adsorption heat transfer coefficient yields good estimation on the experimental data, with the coefficient of determination (R^2) of 0.977 and normalized root mean square error to the mean experimental data (NRMSE) 13.58% achieved. A further investigation of the prediction errors shows that the sources are mainly from the determination of the characteristic parameters of adsorbent-adsorbate pairs. El-Sharkawy [31] pointed out that the LDF model considerably underestimate the rate of water uptake approximately 0.015 kg/kg of silica gel in the early period of the adsorption process, whereas overestimate the rate around 0.003 kg/kg of adsorbent in the later period. The accuracies of the heat of adsorption [32] and the adsorption isotherm equations also contribute to the error. The accuracy of the local adsorption heat transfer coefficient can be further improved if more precise adsorption characteristic equations are applied.

6. CONCLUSION

This work presented the transient heat and mass transfer of silica gel coated heat exchangers in water vapor adsorption processes at sub-atmospheric pressures and assorted temperatures. It is found that the influence of the thermal mass effect is significant for the adsorbent-adsorbate interaction layer and fins at the initial period, and this is the major factor to deviate the transient overall and local adsorption heat transfer coefficients. The remaining are attributed to fluid resistances and tube wall. These ratio proportions of thermal resistances are found to be of slightly different order at the steady-state cooling processes where the fluid resistances becomes the second largest contributor. Based on the experiments, a correlation was proposed to predict the local adsorption heat transfer coefficient and it has good

agreement with the experimental data with the R^2 value 0.977 and NRMSE error is less than 13.58%.

ACKNOWLEDGEMENTS

The authors gratefully acknowledge the National Research Foundation Singapore (grant WBS No. R-265-000-466-281) and King Abdullah University of Science and Technology (grant No. 7000000411) for the financial support to the present research work.

REFERENCES

[1] A. Li, A. B. Ismail, K. Thu, K. C. Ng, and W. S. Loh, "Performance evaluation of a zeolite–water adsorption chiller with entropy analysis of thermodynamic insight," *Applied Energy*, vol. 130, pp. 702-711, 2014.

[2] B. Choudhury, B. B. Saha, P. K. Chatterjee, and J. P. Sarkar, "An overview of developments in adsorption refrigeration systems towards a sustainable way of cooling," *Applied Energy*, vol. 104, pp. 554-567, 2013.

[3] M. W. Shahzad, K. C. Ng, K. Thu, and W. G. Chun, "Multi Effect Desalination and Adsorption Desalination (MEDAD) Cycle," in *lnternational Symposium on Innovative Materials for Processes in Energy Systems 2013*, Fukuoka, Japan, 2013, pp. 115-119.

[4] K. C. Ng, K. Thu, S. J. Oh, A. Li, M. W. Shahzad, and A. B. Ismail, "Recent developments in thermally-driven seawater desalination: Energy efficiency improvement by hybridization of the MED and AD cycles," *Desalination*, vol. 356, pp. 255-270, 2015.

[5] W. S. Loh, K. A. Rahman, K. C. Ng, B. B. Saha, and A. Chakraborty, "Parametric studies of charging and discharging in adsorbed natural gas vessel using activated carbon," *Modern Physics Letters B*, vol. 24, pp. 1421-1424, 2010.

[6] K. A. Rahman, W. S. Loh, A. Chakraborty, B. B. Saha, W. G. Chun, and K. C. Ng, "Thermal enhancement of charge and discharge cycles for adsorbed natural gas storage," *Applied Thermal Engineering*, vol. 31, pp. 1630-1639, 2011.

[7] H. T. Chua, K. C. Ng, W. Wang, C. Yap, and X. L. Wang, "Transient modeling of a two-bed silica gel-water adsorption chiller," *International Journal of Heat and Mass Transfer*, vol. 47, pp. 659-669, 2004.

[8] K. C. Ng, K. Thu, B. B. Saha, and A. Chakraborty, "Study on a waste heat-driven adsorption cooling cum desalination cycle," *International Journal of Refrigeration,* vol. 35, pp. 685-693, 2012.

[9] K. Thu, B. B. Saha, A. Chakraborty, W. G. Chun, and K. C. Ng, "Study on an advanced adsorption desalination cycle with evaporator–condenser heat recovery circuit," *International Journal of Heat and Mass Transfer,* vol. 54, pp. 43-51, 2011.

[10] M. Schicktanz and T. Núñez, "Modelling of an adsorption chiller for dynamic system simulation," *International Journal of Refrigeration,* vol. 32, pp. 588-595, 2009.

[11] S. Li and J. Wu, "Theoretical research of a silica gel–water adsorption chiller in a micro combined cooling, heating and power (CCHP) system," *Applied Energy,* vol. 86, pp. 958-967, 2009.

[12] U. Mayer, M. Groll, and W. Supper, "Heat and mass transfer in metal hydride reaction beds: experimental and theoretical results," *Journal of the Less Common Metals,* vol. 131, pp. 235-244, 1987.

[13] H. Bjurström, E. Karawacki, and B. Carlsson, "Thermal conductivity of a microporous particulate medium: moist silica gel," *International Journal of Heat and Mass Transfer,* vol. 27, pp. 2025-2036, 1984.

[14] E. Tsotsas and H. Martin, "Thermal conductivity of packed beds: a review," *Chemical Engineering and Processing: Process Intensification,* vol. 22, pp. 19-37, 1987.

[15] V. V. Murashov and M. A. White, "Thermal properties of zeolites: effective thermal conductivity of dehydrated powdered zeolite 4A," *Materials chemistry and physics,* vol. 75, pp. 178-180, 2002.

[16] T. Yan, T. X. Li, R. Z. Wang, and R. Jia, "Experimental investigation on the ammonia adsorption and heat transfer characteristics of the packed multi-walled carbon nanotubes," *Applied Thermal Engineering,* vol. 77, pp. 20-29, 2/25/ 2015.

[17] A. Freni, M. Tokarev, G. Restuccia, A. Okunev, and Y. I. Aristov, "Thermal conductivity of selective water sorbents under the working conditions of a sorption chiller," *Applied Thermal Engineering,* vol. 22, pp. 1631-1642, 2002.

[18] E. Hu, D.-S. Zhu, X.-Y. Sang, L. Wang, and Y.-K. Tan, "Enhancement of thermal conductivity by using polymer-zeolite in solid adsorption heat pumps," *Journal of heat transfer,* vol. 119, pp. 627-629, 1997.

[19] L. Wang, D. Zhu, and Y. Tan, "Heat transfer enhancement on the adsorber of adsorption heat pump," *Adsorption,* vol. 5, pp. 279-286, 1999.

[20] T.-H. Eun, H.-K. Song, J. Hun Han, K.-H. Lee, and J.-N. Kim, "Enhancement of heat and mass transfer in silica-expanded graphite composite blocks for adsorption heat pumps: Part I. Characterization of the composite blocks," *International Journal of Refrigeration,* vol. 23, pp. 64-73, 2000.

[21] A. Basile, G. Cacciola, C. Colella, L. Mercadante, and M. Pansini, "Thermal conductivity of natural zeolite-PTFE composites," *Heat Recovery Systems and CHP,* vol. 12, pp. 497-503, 1992.

[22] A. Li, A. B. Ismail, K. Thu, M. W. Shahzad, K. C. Ng, and B. B. Saha, "Formulation of water equilibrium uptakes on silica gel and ferroaluminophosphate zeolite for adsorption cooling and desalination applications," *Evergreen,* vol. 1, pp. 37-45, 2014.

[23] A. B. Ismail, A. Li, K. Thu, K. C. Ng, and W. Chun, "On the thermodynamics of refrigerant + heterogeneous solid surfaces adsorption," *Langmuir,* vol. 29, pp. 14494-14502, 2013.

[24] M. W. Shahzad, A. Myat, W. G. Chun, and K. C. Ng, "Bubble-assisted film evaporation correlation for saline water at sub-atmospheric pressures in horizontal-tube evaporator," *Applied Thermal Engineering,* vol. 50, pp. 670-676, 2013.

[25] A. F. Mills, *Heat and Mass Transfer*: CRC Press, 1995.

[26] T. E. Schmidt, "Heat transfer calculations for extended surfaces," *Refrigerating Engineering*, vol. 57, pp. 351-357, 1949.

[27] C.-C. Wang, R. L. Webb, and K.-Y. Chi, "Data reduction for air-side performance of fin-and-tube heat exchangers," *Experimental Thermal and Fluid Science*, vol. 21, pp. 218-226, 2000.

[28] C.-C. Wang, Y.-c. Hsieh, and Y.-t. Lin, "Performance of plate finned tube heat exchangers under dehumidifying conditions," *Journal of heat transfer*, vol. 119, pp. 109-117, 1997.

[29] K. T. Hong and R. L. Webb, "Calculation of fin efficiency for wet and dry fins," *HVAC&R Research*, vol. 2, pp. 27-41, 1996.

[30] H. Moschiano, W. Dabney, R. S. Johnson, and L. Placek, "Thermal and electrical characterizatio of PAA and HEC gel used in MRI testing of active and passive medical implants," in *Proceedings of International Society for Magnetic Resonance in Medicine 18*, Sweden, 2010, p. 18.

[31] I. I. El-Sharkawy, "On the linear driving force approximation for adsorption cooling applications," *International Journal of Refrigeration*, vol. 34, pp. 667-673, 2011.

[32] A. B. Ismail, "Experimental and theoretical studies on adsorption chillers driven by waste heat and propane," Doctor of Philosophy, Department of Mechanical Engineering, National University of Singapore, Singapore, 2013.

Figure 1: Schematic representation of the adsorption heat transfer experimental apparatus

Figure 2: Specifications of the silica gel coated heat exchanger, including (a) dimensions; (b) location of the temperature thermistors; and (c) a pictorial view of the heat exchanger.

Figure 3: Thermal layers encountered in an adsorbent embedded heat exchanger during adsorption processes

Figure 4: Temporal temperature difference between the inlet cooling water $T_{i,cw}$ and the silica gel average T_{ads} at various cooling water temperatures for the silica gel coated heat exchanger

Figure 5: Temporal overall heat transfer coefficient of the silica gel coated heat exchanger at various cooling water temperatures

Figure 6: Temporal variation of the surface efficiency of the silica gel coated heat exchanger during adsorption processes at various cooling water temperatures

Figure 7: Temporal local adsorption heat transfer coefficient of the silica gel coated heat exchanger during adsorption processes at various cooling water temperatures

Figure 8: Comparison of temporal overall and local adsorption heat transfer coefficient of the silica gel coated heat exchanger during adsorption process at 30 ^{o}C cooling water temperature

Figure 9: Temporal thermal resistance of various layers in the silica gel coated heat exchanger during adsorption process at 30 ^{o}C cooling water temperature

Figure 10: Percentage contribution of each layer's thermal resistance in the silica gel coated heat exchanger during adsorption process at 30 ^{o}C cooling water temperature

Figure 11: Percentage contribution of the adsorption layer from thermal mass effect in the silica gel coated heat exchanger during adsorption process at 30 ^{o}C cooling water temperature

Figure 12: Percentage contribution of the fin from thermal mass effect in the silica gel coated heat exchanger during adsorption process at 30 ^{o}C cooling water temperature

Figure 13: Illustration of heat flow on the heat exchanger in a typical adsorption process

Figure 14: Predicted results of Equation 23 on the local adsorption heat transfer coefficient of the silica gel coated heat exchanger during water adsorption processes at cooling water temperature (a) 25 ^{o}C, (b) 30 ^{o}C, (c) 35 ^{o}C, and (d) 40 ^{o}C. The experimental results are displayed in 10% error bars

Table 1: Testing conditions of the adsorption heat transfer experiment

Parameter	Value
Inlet temperature of cooling water	25 ^{o}C, 30 ^{o}C, 35 ^{o}C and 40 ^{o}C
Cooling water flow-rate	1 LPM
Evaporation temperature in evaporator	5.6 ^{o}C
Adsorption period	320 s

Table 2: Summary on the equations of adsorption characteristic parameters

Equations of Adsorption Characteristics
Adsorption kinetics (Linear Driving Force model) • *Instantaneous uptake of adsorbate* $q(t) = q^{*} - \left[q^{*} - q_{ini} \right] \exp\left(-\kappa t\right)$ • *Rate of instantaneous uptake of adsorbate* $\frac{dq(t)}{dt} = \kappa \left[q^{*} - q_{ini} \right] \exp\left(-\kappa t\right)$ • *Kinetics coefficient* $\kappa = \frac{15 D_{so}}{R_p^2} \exp\left(-\frac{E_a}{R T_{ads}(t)} \right)$
Equilibrium uptake (Adsorption isotherms) [22] $\frac{q^{*}}{q_0} = \frac{A\phi \exp(\beta \frac{P}{P_s}) \frac{P}{P_s} + C \frac{P}{P_s}}{\left\{ 1 + \phi \exp(\beta \frac{P}{P_s}) \frac{P}{P_s} \right\}^{t}}$ where, $\beta = \exp\left(\frac{E_c}{R T_{ads}(t)} \right)$ $A = \frac{\left[1 + \phi \exp(\beta) \right]^{t} - C}{\phi \exp(\beta)}$
Heat of adsorption [23] $Q_{st,ads} = -P\left(v_g - v_a\right) \ln\left(KP\right)$
Specific heat of adsorbed phase [23] $Cp_{\alpha} = Cp_g + P \ln\left(KP\right) \left[2 \left(\frac{\partial v_g}{\partial T} \right)_P - \frac{v_g}{T} \right] - \frac{\left[P \ln\left(KP\right) \right]^2}{T} \left(\frac{\partial v_g}{\partial P} \right)_P$

Table 3: Summary on the equations of heat exchanger surface efficiency

Equations of Heat Exchanger Surface Efficiency
Surface efficiency
$\eta = 1 - \frac{A_{fin}}{A}\left(1 - \eta_{fin}\right)$ where, $\eta_{fin} = \frac{\tanh\left(\xi r_o \phi\right)}{\xi r_o \phi}$,
$\xi = \sqrt{\frac{2h_{t,ads}}{k_{fin}\delta_{fin}}}$ and, $\phi = \left(\frac{R_{eq}}{r_o} - 1\right)\left[1 + 0.35\ln\left(\frac{R_{eq}}{r_o}\right)\right]$
Geometric factors
$\frac{R_{eq}}{r_o} = \begin{cases} 1.27\frac{X_M}{r_o}\left(\frac{X_L}{X_M} - 0.3\right)^{1/2} & \text{for staggered tubes} \\ 1.28\frac{X_M}{r_o}\left(\frac{X_L}{X_M} - 0.2\right)^{1/2} & \text{for inline and one-row tubes} \end{cases}$
where, $X_L = \begin{cases} \sqrt{\left(P_t/2\right)^2 + P_l^2} & \text{for staggered tubes} \\ P_l/2 & \text{for inline and one-row tubes} \end{cases}$
and, $X_M = P_t/2$

Table 4: Value of parameters in the calculation of local adsorption heat transfer coefficient

Parameters	**Values**	**Parameters**	**Values**
Tube (copper)			
Inner diameter, d_i [mm]	7.747	Thermal conductivity, k_{tw} [W/m.K]	385
Outer diameter, d_o [mm]	9.525	Thermal mass, $M_{tw}Cp_{tw}$ [kJ/K]	0.035
Length, L_{tw} [m]	0.377	Total surface area, A [m^2]	0.066
Fin (copper)			
Fin thickness, δ_{fin} [mm]	0.25	Thermal conductivity, k_{fin} [W/m.K]	385
Fin area, A_{fin} [m^2]	0.058	Thermal mass, $M_{fin}Cp_{fin}$ [kJ/K]	0.04

Table 5: Properties of water and silica gel type RD powder with 3.3 adsorbent wt% HEC

Parameters	Values	Parameters	Values
Adsorbent (silica gel RD powder)			
M_{sg} [kg]	0.0374	Cp_{sg} [kJ/kg.K]	0.921
ρ_{sg} [kg/m^3]	800	k_{sg} [W/m.K]	0.198
δ_{sg} [mm]	0.707		
Binder (HEC)			
M_b [kg]	1.235×10^{-3}	Cp_b [kJ/kg.K]	3.851
Adsorption isotherms			
q_0 [kg/kg]	0.455	E_c [kJ/kg]	378.1
ϕ [-]	$8.27\text{x}10^{-4}$	C [-]	1.064
t [-]	0.975		
Kinetics constant (κ) & Heat of adsorption (Q_{st})			
D_{so} [m^2/s]	2.54×10^{-4}	R_p [mm]	0.205
E_a [kJ/kmol]	4.2×10^{-4}	K [kPa^{-1}]	7.182×10^{-9}